Inorganic Chemistry
Article

Inorg. Chem. **2009**, *48*, 10643–10651 **10643**
DOI: 10.1021/ic901337r

A Mixed-Valent Pentanuclear $Cu^{II}_4Cu^{I}$ Compound Containing a Radical-Anion Ligand

Tiddo J. Mooibroek,[†] Guillem Aromí,[*,‡] Manuel Quesada,[†] Olivier Roubeau,[§] Patrick Gamez,[*,†] Serena DeBeer George,[∥] Joris van Slageren,[⊥,▽] Shadi Yasin,[▽] Eliseo Ruiz,[‡] and Jan Reedijk[†]

[†]*Contribution from the Leiden Institute of Chemistry, Leiden University, P.O. Box 9502, 2300 RA Leiden, The Netherlands,* [‡]*Departament de Química Inorgànica, Universitat de Barcelona, Diagonal 467, 08028 Barcelona, Spain,* [§]*Université Bordeaux 1, Centre de Recherche Paul Pascal-CNRS, 115 avenue du dr. A. Schweitzer, 33600 Pessac, France,* [∥]*Department of Chemistry & Chemical Biology, Baker Laboratory, Cornell University, Ithaca, New York 14853,* [⊥]*University of Nottingham, School of Chemistry, Nottingham NG7 2RD, United Kingdom, and* [▽]*1. Physikalisches Institut, Universität Stuttgart, Pfaffenwaldring 57, D-70550 Stuttgart, Germany*

Received July 10, 2009

Reaction of 2,4-(2,2′-dipyridylamino)-6-(2-pyridylhydrazino)-1,3,5-triazine, abbreviated dppht (**5**), with copper(II) chloride in methanol yields a mixed-valent $Cu^{II}_4Cu^{I}$ compound (**6**), also involving the presence of a radical anion. The single-crystal structure determination for $[Cu_5(\mathbf{5^M})(\mathbf{5^{MR}})Cl_8]$ (**6**) reveals that the original dppht ligand (**5**) has been monochlorinated at one of its pyridine rings and oxidized at its hydrazyl moiety, generating the ligand 2,4-(2,2′-dipyridylamino)-6-(2-(5-chloropyridyl)azo)-1,3,5-triazine ($\mathbf{5^M}$). Moreover, the molecular structure of **6** indicates that one of the two coordinated ligands $\mathbf{5^M}$ is in a radical-anion state, symbolized as $\mathbf{5^{MR}}$, characterized by a typical N−N bond length of about 1.33 Å for a one-electron reduced azo group. The nature of this unique $[Cu^{II}_4Cu^{I}(\text{radical})]$ assembly is corroborated by X-ray absorption spectroscopy, electron paramagnetic resonance, and magnetic susceptibility measurements. Density-functional theory calculations are consistent with the unprecedented structural features and support the spectroscopic data.

Introduction

The preparation and study of mixed-valence copper(I,II) coordination compounds derived from multifunctional bridging ligands is an area of topical interest,[1,2] due to the relevance of such species as biomimetic model systems,[3−5] and owing to their potentially interesting magnetic or electronic (electron transfer) properties.[6−9] Different approaches can be envisaged to synthesize mixed-valence copper(I,II) complexes.[10] Most $Cu^{I,II}$ materials currently reported in the literature are obtained from copper(II) sources, by reduction of some of the metal centers under solvothermal, basic conditions.[11−13] A second possibility is to design ligands capable of accommodating copper ions in two different redox states.[14] The goal is then to access ligands which can support a variety of coordination modes, allowing the simultaneous coordination of added copper(I) and copper(II) ions.[15] An alternative pathway to mixed-valence copper(I,II) species is to use azo-based ligands.[16] For instance, hydrazino derivatives are known to act as reducing agents,[17] and the simple reaction of hydrazine with copper(II) chloride in acidic aqueous solution produces four different copper compounds, including a mixed Cu^{I}/Cu^{II} species.[18] Recently, Kaim et al.

*To whom correspondence should be addressed. E-mail: p.gamez@chem.leidenuniv.nl (P.G.), guillem.aromi@qi.ub.es (G.A.).

(1) Demadis, K. D.; Hartshorn, C. M.; Meyer, T. *J. Chem. Rev.* **2001**, *101*, 2655–2685.
(2) Kaim, W.; Klein, A.; Glockle, M. *Acc. Chem. Res.* **2000**, *33*, 755–763.
(3) Kuzelka, J.; Mukhopadhyay, S.; Spingler, B.; Lippard, S. J. *Inorg. Chem.* **2004**, *43*, 1751–1761.
(4) He, C.; Lippard, S. J. *Inorg. Chem.* **2000**, *39*, 5225–5231.
(5) Lu, Y. *Angew. Chem., Int. Ed.* **2006**, *45*, 5588–5601.
(6) Zhang, X. M.; Tong, M. L.; Gong, M. L.; Lee, H. K.; Luo, L.; Li, K. F.; Tong, Y. X.; Chen, X. M. *Chem.—Eur. J.* **2002**, *8*, 3187–3194.
(7) Zhang, X. M.; Tong, M. L.; Chen, X. M. *Angew. Chem., Int. Ed.* **2002**, *41*, 1029–1031.
(8) Harding, C.; McKee, V.; Nelson, J. *J. Am. Chem. Soc.* **1991**, *113*, 9684–9685.
(9) Houser, R. P.; Young, V. G.; Tolman, W. B. *J. Am. Chem. Soc.* **1996**, *118*, 2101–2102.
(10) Dunajjurco, M.; Ondrejovic, G.; Melnik, M.; Garaj, J. *Coord. Chem. Rev.* **1988**, *83*, 1–28.
(11) Chen, X. M.; Tong, M. L. *Acc. Chem. Res.* **2007**, *40*, 162–170.
(12) Huang, X. C.; Zhang, J. P.; Lin, Y. Y.; Yu, X. L.; Chen, X. M. *Chem. Commun.* **2004**, 1100–1101.
(13) Zhang, X. M.; Fang, R. Q. *Inorg. Chem.* **2005**, *44*, 3955–3959.
(14) Brooker, S.; Ewing, J. D.; Ronson, T. K.; Harding, C. J.; Nelson, J.; Speed, D. J. *Inorg. Chem.* **2003**, *42*, 2764–2773.
(15) Veauthier, J. M.; Tomat, E.; Lynch, V. M.; Sessler, J. L.; Mirsaidov, U.; Markert, J. T. *Inorg. Chem.* **2005**, *44*, 6736–6743.
(16) Baker, R. J.; Szymansk, J.; Nyburg, S. C. *Inorg. Chem.* **1971**, *10*, 138–146.
(17) Borodko, Y. G.; Efimov, O. N.; Panov, V. B.; Shulga, Y. M. *Izv. Akad. Nauk SSSR, Ser. Khim.* **1973**, 936–937.
(18) Brown, D. B.; Donner, J. A.; Hall, J. W.; Wilson, S. R.; Wilson, R. B.; Hodgson, D. J.; Hatfield, W. E. *Inorg. Chem.* **1979**, *18*, 2635–2641.

Published on Web 10/09/2009

Chart 1

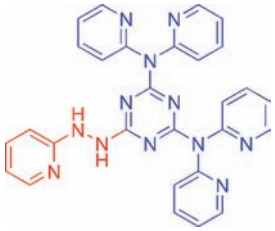

theoretically demonstrated that the ligand 2,2′-azobispyridine (abpy) can evolve to a bridging radical anion ligand, able to stabilize mixed-valent complexes.[19−21] Various examples of mixed-valence ruthenium(II,III) complexes coordinated by such azo-type radical anion ligands have been described.[22,23] Dicopper(I) coordination compounds exhibiting radical-anionic ligands have been evidenced by spectroscopic studies,[24,25] and the first crystallographic proof of a dicopper(I) complex bearing a stable azoaromatic radical anion ligand was reported already in 1998.[26] However, to the best of our knowledge, X-ray structural proof of a radical anion within a mixed-valence copper(I,II) coordination has not been reported so far.

In the present study, a new, bifunctional ligand, that is, 2,4-(2,2′-dipyridylamino)-6-(2-pyridylhydrazino)-1,3,5-triazine (dppht; Chart 1) has been used with the expectation of preparing a mixed-valence copper(I,II) complex. In relation to this, it must be noted that the triazine-based ligand dppht presents two different functional parts, indicated by different colors in Chart 1. The unit represented in blue is known to efficiently bind copper(II) ions.[27−29] The hydrazino group depicted in red (Chart 1) is expected to act as a reducing agent, thus promoting the in situ formation of copper(I) ions. In addition, the copper(II)-mediated oxidation (and deprotonation) of the ligand dppht (Scheme S1, Supporting Information) may lead to the generation of azoaromatic radical anions, given that the oxidized ligand resembles the abpy ligand investigated by Kaim et al. (Scheme S1).[20] Actually, the reaction of copper(II) chloride with dppht in methanol produces a mixed-valence copper(I,II) complex. Moreover, the obtained deep, dark-purple-colored compound is characterized by the presence of one stable chlorinated radical-anion ligand and one neutral chlorinated ligand, as evidenced by X-ray diffraction analyses and diverse spectroscopic techniques and supported by theoretical calculations.

Experimental Section

Materials and Methods. Solvents and chemicals were commercially available as A.R. grade and used as received. All reactions were performed under an inert atmosphere of argon, and the purifications were commonly performed in the air.

Proton magnetic resonance (^{1}H NMR) and carbon nuclear magnetic resonance (^{13}C NMR) spectra were recorded on a DPX 300 Bruker (300 MHz) spectrometer at 25 °C. Proton and carbon chemical shifts are expressed in parts per million (ppm, δ scale) and are referenced to the solvent peak. Infrared spectra were recorded using a Perkin-Elmer Paragon 1000 spectrophotometer equipped with a Golden Gate Diamond ATR as a sample support, and data are represented as the frequency of absorption (cm^{-1}). Ligand field spectra of the solid compounds were recorded on a Perkin-Elmer Lambda 900 UV−vis−NIR spectrometer in the diffuse reflectance mode with MgO as a reference, and using a 1 nm interval.

C, H, and N analyses were carried out using an automatic Perkin-Elmer 2400 Series II CHNS/O analyzer. Electrospray ionization (ESI) mass spectroscopy was carried out using a Finnigan AQA Mass Spectrometer equipped with an ESI source. Sample solutions (10 μL of a 1 mg mL^{-1} solution) were introduced in the ESI source by using a Dionex ASI-100 automated sampler injector and an eluent running at 0.2 mL min^{-1}. The chloride analysis was performed by potentiometric titrations using a freshly prepared $AgNO_3$ solution (0.0197 M) and determined with a Ag electrode and a Ag/AgCl (3 M KCl) reference electrode (E = 0.205 V). The signals were recorded using a Kip&Zonen BD 40 analogue recorder, operated at 200 mV (see the Supporting Information for the general method used for the potentiometric titrations).

X-band EPR spectra were recorded on a Bruker ESP 300 X-band spectrometer equipped with a continuous flow helium cryostat. Variable-temperature and -field magnetic measurements were performed in the range 2−300 K using a Quantum Design MPMS-7XL SQUID magnetometer in fields of 0−7 T. Corrections for diamagnetic portions of the complex, deduced from Pascal's tables,[30] and for the sample holder were applied.

XAS Data Collection and Analysis. XAS data were measured at the Stanford Synchrotron Radiation Laboratory (ring conditions of 3.0 GeV and 60−100 mA) on unfocused bend magnet beamline 2−3. A Si(220) monochromator was utilized for energy selection. The monochromator was detuned 50% to minimize higher harmonics. Complex **6** was prepared as a solid in boron nitride, pressed into a pellet, and sealed in a 38 μm Kapton tape window in a 1 mm aluminum spacer. The sample was maintained at 10 K during data collection using an Oxford Instruments CF1208 continuous flow liquid helium cryostat. Data were measured in the transmission mode. Internal energy calibrations were performed by simultaneous measurement of a Cu reference foil placed between a second and third ionization chamber. The first inflection point was assigned to 8980.3 eV. Data represent two to three scan averages and were processed by fitting a second-order polynomial to the pre-edge region and subtracting this background from the entire spectrum. A three-region cubic spline was used to model the smooth background above the edge. The data were normalized by subtracting the spline and normalizing the postedge 1.0.

Synthesis of 2,4-(2,2′-Dipyridylamino)-6-chloro-1,3,5-triazine (3). This compound was synthesized according to a procedure earlier reported to prepare related derivatives.[31] 2,4,6-Trichloro-[1,3,5]triazine (**1**; 5.16 g, 28.21 mmol) was dissolved in 52 mL of tetrahydrofuran in a two-necked round-bottomed flask. A total of 2 equiv (7.28 g, 56.40 mmol) of *N*,*N*-diisopropylethylamine (DIPEA) was added, and the mixture was cooled to 0 °C

(19) Hellmann, M.; Frantz, S.; Kaim, W.; Fiedler, J.; Duboc, C. *Inorg. Chim. Acta* **2006**, *359*, 821–829.
(20) Sarkar, B.; Patra, S.; Fiedler, J.; Sunoj, R. B.; Janardanan, D.; Mobin, S. M.; Niemeyer, M.; Lahiri, G. K.; Kaim, W. *Angew. Chem., Int. Ed.* **2005**, *44*, 5655–5658.
(21) Kaim, W.; Lahiri, G. K. *Angew. Chem., Int. Ed.* **2007**, *46*, 1778–1796.
(22) Kaim, W.; Sarkar, B. *Coord. Chem. Rev.* **2007**, *251*, 584–594.
(23) Kasack, V.; Kaim, W.; Binder, H.; Jordanov, J.; Roth, E. *Inorg. Chem.* **1995**, *34*, 1924–1933.
(24) Barra, A. L.; Brunel, L. C.; Baumann, F.; Schwach, M.; Moscherosch, M.; Kaim, W. *J. Chem. Soc., Dalton Trans.* **1999**, 3855–3857.
(25) Glockle, M.; Hubler, K.; Kummerer, H. J.; Denninger, G.; Kaim, W. *Inorg. Chem.* **2001**, *40*, 2263–2269.
(26) Doslik, N.; Sixt, T.; Kaim, W. *Angew. Chem., Int. Ed.* **1998**, *37*, 2403–2404.
(27) Gamez, P.; Reedijk, J. *Eur. J. Inorg. Chem.* **2006**, 29–42.
(28) Demeshko, S.; Dechert, S.; Meyer, F. *J. Am. Chem. Soc.* **2004**, *126*, 4508–4509.
(29) de Hoog, P.; Gamez, P.; Mutikainen, H.; Turpeinen, U.; Reedijk, J. *Angew. Chem., Int. Ed.* **2004**, *43*, 5815–5817.
(30) Kahn, O. *Molecular Magnetism*; Wiley-VCH: New York, 1993.
(31) de Hoog, P.; Gamez, P.; Driessen, W. L.; Reedijk, J. *Tetrahedron Lett.* **2002**, *43*, 6783–6786.

(ice bath). Dipyridin-2-ylamine (**2**; 9.63 g, 56.29 mmol) was then added portionwise. After completion of the addition, the transparent reaction mixture was warmed to room temperature and subsequently heated under reflux for 48 h. The yellow precipitate that formed was isolated on a glass filter and washed with THF (2×20 mL) and ethanol (3×25 mL) to remove the byproduct *N*,*N*-diisopropylethylamine hydrochloride. The crude compound was purified by column chromatography (300 g silica, Ø = 5 cm, CH_2Cl_2/MeOH/NH_3 (94.5:5:0.5) as eluent). Product **3** was dried overnight at 100 °C under reduced pressure. Yield: 8.84 g or 69%. ^{1}H NMR (300 MHz, $CDCl_3$): δ 7.11 (dd, 4H, 4-py-H), 7.46 (d, 4H, 6-py-H), 7.65 (dd, 4H, 5-py-H), 8.37 (d, 4H, 3-py-H) ppm. ^{13}C NMR (75 MHz, DMSO-d6 = solvent): δ 121.8 (6-py-C), 122.8 (4-py-C), 137.8 (5-py-C), 148.3 (3-py-C), 154.1 (1-py-C), 165.4 (4,6-triaz-C), 168.9 (2-triaz-C) ppm. IR (neat): ν 744, 774, 800, 996, 1218, 1432, 1458, 1471 (2-substituted pyridine), 1497, 1550, 1590 (triazine); 616, 624, 657, 660, 668, 684, 724 (C−Cl), 1120, 1146, 1258, 1388 (tertiary aromatic amine); 826, 889, 1019, 1051, 1654 (C−C and C−N stretch) cm^{-1}. Anal. Calcd for $C_{23}H_{16}ClN_9$: C, 60.86; H, 3.55; N, 27.77. Found: C, 60.13; H, 3.43; N, 28.50. MS (ESI): *m*/*z* 453.7 (M^+).

Synthesis of 2,4-(2,2′-Dipyridylamino)-6-(2-pyridylhydrazino)-1,3,5-triazine (5; dppht). 2-(Pyridin-2-yl)hydrazine (**4**; 1.02 g, 9.31 mmol) was dissolved in tetrahydrofuran (50 mL) under argon in a two-necked round-bottomed flask, and 1 equiv of DIPEA (1.20 g, 9.31 mmol) was added to the solution. A total of 1 equiv of **3** (4.22 g, 9.31 mmol) was subsequently added, portionwise, to the mixture. After completion of the addition, the reaction mixture was refluxed for 6 h. After this, the reaction mixture was cooled down to 4 °C, and a yellow precipitate was collected by filtration. The *N*,*N*-diisopropylethylamine hydrochloride was removed upon washing with cold THF (2×10 mL). The pure product **5** (light yellow powder) obtained was dried under reduced pressure. Yield: 3.19 g or 65%. ^{1}H NMR (300 MHz, $CDCl_3$): δ 6.67 (d, 5H, 0.028 Hz, 6-py-H), 6.81 (dd, 5H, 0.016 Hz, 4-py-H), 6.83 (s, 2H, hydr-H), 7.54 (dd, 5H, 0.026 Hz, 5py-H), 8.13 (d, 5H, 0.017 Hz, 3-py-H) ppm. ^{13}C NMR (75 MHz, $CDCl_3$): δ 107.1 (4-py-hydr-C), 116.0 (6-py-hydr-C), 120.8 (4-py-C), 122.9 (6-py-C), 137.1 (5-py-C), 137.8 (5-py-hydr-C), 147.8 (3-py-hydr-C), 148.3 (3-py-C) ppm. IR (neat): ν 1428, 1456, 809, 996, 738, 773 (2-substituted pyridine), 1538, 1588 (triazine), 1362 (tertiary aromatic amine), 880, 1050, 1654 (C−C and C−N stretch), 1237, 1308, 1362 (N−H hydrazine) cm^{-1} (Figure S1, Supporting Information). Anal. Calcd for $C_{28}H_{22}N_{12}$: C, 63.87; H, 4.21; N, 31.92. Found: C, 63.82; H, 4.72; N, 31.45. MS (ESI): *m*/*z* 526.6 (M^+).

Synthesis of [Cu_5(5^M)(5^{MR})Cl_8] (6). A solution of dppht (**5**, 181.5 mg, 0.345 mmol) in 20 mL of methanol was added to a solution of $CuCl_2 \cdot 2H_2O$ (146.9 mg, 0.862 mmol) in 20 mL of methanol. The resulting dark brown reaction mixture (in which the Cu/ligand ratio was 2.5:1) was left unperturbed for the slow evaporation of the solvent. After two days, dark purple parallelepiped crystals of **6** were obtained. Yield: 64.4 mg or 22% (based on dppht). Anal. Calcd for $C_{56}H_{38}Cl_{10}Cu_5N_{24} \cdot 2H_2O$: C, 38.3; H, 2.4; N, 19.2; Cl, 20.2. Found: C, 38.7; H, 2.4; N, 19.0; Cl, 19.1. IR (neat): ν cm^{-1} 3076, 1603, 1584, 1557, 1526, 1491, 1387, 1234, 1158, 1115, 1016, 771, 668, 420 cm^{-1} (Figure S2, Supporting Information). Diffuse reflectance: the almost black compound **6** exhibits a continuous absorption over the whole spectrum range (Figure S3, Supporting Information).

X-Ray Crystallography. Single-Crystal X-ray Diffraction. X-ray crystallographic data were collected at 293 K on a Nonius Kappa CCD diffractometer with graphite-monochromated Mo Kα radiation (λ = 0.71073 Å). A suitable small dark plate crystal was affixed to the end of a glass fiber using silicone grease and transferred to the goniostat. DENZO-SMN was used for data integration and SCALEPACK corrected data for Lorentz-polarization effects.[32] The structure was solved by direct methods and refined by a full-matrix least-squares method on F^2 using the SHELXTL crystallographic software package.[33,34] Data were cut at 0.95 Å as then $I/\sigma(I) < 1.5$. All crystals tested showed such poor diffraction, probably related to diffuse solvent areas. Indeed, remaining weak residual electron density lying in voids in between the Cu_5 units could not be modeled satisfactorily as solvent lattice molecules. The corresponding voids were therefore analyzed and taken into account with PLATON/SQUEEZE,[35] resulting in significant improvements in both R1 (1.4%) and wR2 (2%) factors. Selected bond distances and angles are listed in Table S1 (Supporting Information), and crystallographic data for **6** are given in Table S2 (Supporting Information). Crystallographic data (excluding structure factors) for the structure reported have been deposited with the Cambridge Crystallographic Data Centre as supplementary publication CCDC no. 737831.

Computational Details. The calculations to optimize the structure of the studied complex were carried out using the 2.0 version of the SIESTA code (Spanish Initiative for Electronic Simulations with Thousands of Atoms).[36] We employed the generalized-gradient approximation functional proposed by Perdew, Burke, and Erzernhof (PBE).[37] Only valence electrons are included in the calculations, as in the case of the plane waves, the cores being replaced by norm-conserving scalar relativistic pseudopotentials factorized in the Kleinman-Bylander form.[38] These pseudopotentials are generated according to the procedure proposed by Trouiller and Martins.[39] The core radii for the s, p, and d components for copper atoms are all 2.00 au, and we have included partial-core corrections for such atoms to provide a better description of the core region. The cutoff radii were 1.15 for hydrogen and nitrogen atoms, 1.25 for carbon atoms, and 1.60 for chlorine atoms.

A double-ζ numerical basis set was employed, including polarization functions. In these kinds of calculations, there are two key parameters that control the accuracy.[40−42] The numerical wave function is zero at a radius larger than the chosen confinement radius r_c, whose value is different for each atomic orbital. The confinement radius of different orbitals is determined by a single parameter, *the energy shift* that corresponds to the energy increase of the atomic eigenstate due to the confinement. The integrals of the self-consistent terms are calculated with the help of a regular real space grid in which the electron density is projected. The grid spacing is determined by the *maximum kinetic energy* of the plane waves that can be represented in that grid. The values of 50 meV for the energy shift and 250 Ry for the mesh cutoff provide a good compromise between accuracy and the computational cost required to provide an accurate description of the system with tiny energy differences between the ground and excited states.[43]

(32) Otwinowski, Z.; Minor, W. *Methods Enzymol.* **1996**, *276*, 307–326.

(33) Sheldrick, G. M. *SHELXTL*; Bruker AXS Inc.: Madison, WI, 2001.

(34) Sheldrick, G. M. *Acta Crystallogr., Sect. A* **2008**, *64*, 112–122.

(35) Spek, A. L. *PLATON*; Utrecht University: Utrecht, The Netherlands, 2008.

(36) Artacho, E.; Gale, J. D.; García, A.; Junquera, J.; Martin, R. M.; Ordejón, P.; Sánchez-Portal, D.; Soler, J. M. *SIESTA*; The Fundación General de la Universidad Autónoma de Madrid: Madrid, Spain, **2006**.

(37) Perdew, J. P.; Burke, K.; Ernzerhof, M. *Phys. Rev. Lett.* **1996**, *77*, 3865–3868.

(38) Kleinman, L.; Bylander, D. M. *Phys. Rev. Lett.* **1982**, *48*, 1425–1428.

(39) Troullier, N.; Martins, J. L. *Phys. Rev. B* **1991**, *43*, 1993–2006.

(40) Artacho, E.; Sanchez-Portal, D.; Ordejon, P.; Garcia, A.; Soler, J. M. *Phys. Status Solidi B* **1999**, *215*, 809–817.

(41) Sanchez-Portal, D.; Ordejon, P.; Artacho, E.; Soler, J. M. *Int. J. Quantum Chem.* **1997**, *65*, 453–461.

(42) Soler, J. M.; Artacho, E.; Gale, J. D.; Garcia, A.; Junquera, J.; Ordejon, P.; Sanchez-Portal, D. *J. Phys., Condens. Matter* **2002**, *14*, 2745–2779.

(43) Ruiz, E.; Rodriguez-Fortea, A.; Tercero, J.; Cauchy, T.; Massobrio, C. *J. Chem. Phys.* **2005**, 123.

Scheme 1. Synthesis of Ligand **5** (dppht)

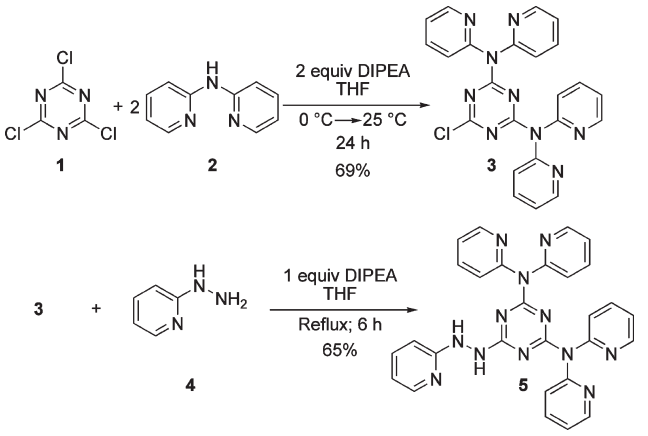

Results and Discussion

Synthesis of 2,4-(2,2′-Dipyridylamino)-6-(2-pyridylhydrazino)-1,3,5-triazine (5; dppht). Compound **5** was prepared via two straightforward steps (Scheme 1), following a procedure earlier reported for the synthesis of related compounds.[31] Thus, the reaction of cyanuric chloride (**1**) with 2 equiv of 2,2′-dipyridylamine (**2**) in tetrahydrofuran leads to the formation of 6-chloro-*N*,*N*,*N*′,*N*′-tetra-(pyridin-2-yl)-1,3,5-triazine-2,4-diamine (**3**), with a yield of 69%. *N*,*N*-DIPEA is used to neutralize the HCl generated during the substitution reaction. The reaction of **3** with 1 equiv of 2-(pyridin-2-yl)hydrazine (**4**) produces the targeted compound **5** with a yield of 65%.

Synthesis of $[Cu_5(5^M)(5^{MR})Cl_8]$ (6). The reaction of 2.5 equiv of copper(II) chloride dihydrate with 1 equiv of ligand **5** (dppht) in methanol produces dark purple crystals of **6** after two days, with a yield of 27% (based on the ligand **5**). The synthesis of compound **6** has been reproduced several times.

Crystal Structure of $[Cu_5(5^M)(5^{MR})Cl_8]$ (6). Single-crystal X-ray studies revealed that **6** crystallizes in the monoclinic space group $P2_1/c$. An ORTEP[44] view of **6** is represented in Figure 1. Selected bond distances and angles are given in Table S1 (Supporting Information), and details for the structure solution and refinement are summarized in Table S2 (Supporting Information). During the crystallization process, the initial ligand **5** has been modified, unexpectedly, to chlorinated species, either the modified ligand 5^M or the radical anion 5^{MR}, depicted in Scheme 2. These modifications and the particular features of these in situ generated ligands are discussed below (see the Ligand Modification section). The core of the pentanuclear compound **6** (Scheme 3) is composed of four different five-coordinated copper(II) ions identified as Cu1, Cu2, Cu3, and Cu5, and one four-coordinated copper(I) ion, that is, Cu4, held together by two chlorinated modified species and a chloride bridge. The presence of mixed-valence species has been confirmed by various techniques, including XAS and supported by theoretical calculations (see corresponding sections below); nevertheless, the bond-valence sum analysis does not allow assigning unequivocally the +1 or +2 oxidation state to the different Cu centers in **6**. The coordination

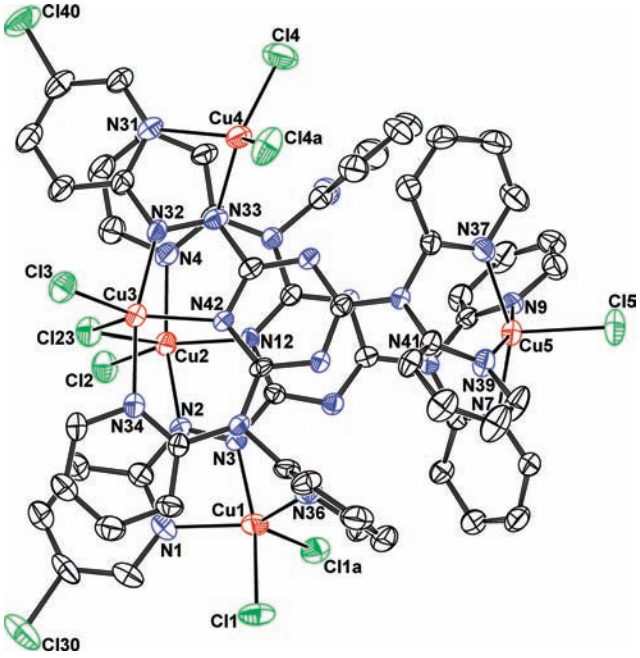

Figure 1. Thermal ellipsoid (30% probability level) plot of **6**. H atoms are omitted for clarity.

Scheme 2. Representation of the Modified 5^M Ligand (left) and 5^{MR} Radical Anion (right)

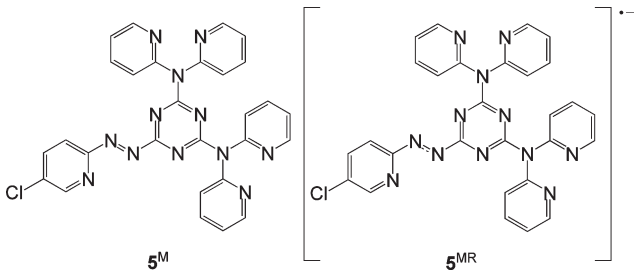

Scheme 3. Magnetic Coupling Scheme in **6** with the Numbering Used in the Text[a]

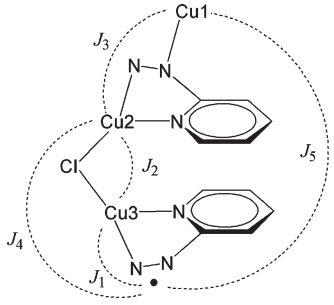

[a] The diamagnetic Cu4 and the Cu5, the latter considered as isolated, are omitted.

geometry around Cu1 is best described as intermediate between trigonal bipyramidal and square pyramidal, with a τ_5 value of 0.59 (τ_5 describes the distortion of the coordination geometry with respect to a trigonal bipyramid and a square-based pyramid; for a perfectly square-pyramidal geometry $\tau_5 = 0$, and $\tau_5 = 1$ for a perfectly trigonal-bipyramidal geometry).[45] The Cu−N and

(44) Spek, A. L. *Platon*; Utrecht University: Utrecht, The Netherlands, 2006.

(45) Addison, A. W.; Rao, T. N.; Reedijk, J.; van Rijn, J.; Verschoor, G. C. *J. Chem. Soc., Dalton Trans.* **1984**, 1349–1356.

Cu−Cl bond distances (Table S1) can be considered as normal, except for Cu−N36, which is particularly long.[46] The coordination angles varying from 78.0(3)° to 162.9(2)° reflect the strong distortion, most likely resulting from both the small bite angle of the azo-pyridine bidentate moiety (N1−Cu1−N3 = 78.0(3)°) and steric constraints due to the $\pi-\pi$ stacking of the two ligands (which are therefore in close contact) coordinating the five copper atoms. The coordination of the pyridine ring containing N36 is also distorted, as indicated by a Cu1−N36−centroid angle strongly deviating from 180° (151.1°). N36 is thus only very weakly coordinated, and the environment of Cu1 in fact resembles that of the Cu(I) in Cu4. The valence of Cu1 is therefore not clearly evidenced by its environment. The coordination environment of Cu2 is best described as a heavily distorted square pyramid (τ_5 = 0.36).[45] The Cu−N and Cu−Cl bond distances (Table S1) are in normal ranges for Cu(II) in this type of coordination geometry.[47] The basal coordination angles deviate significantly from the ideal value of 90° (these angles vary from 78.6(3) to 97.7(2) for Cu2), arising from the small bite angle of the bidentate N2, N12 unit (see Figure 1; N2−Cu2−N12 = 78.6(3)°), and from particular structural features involving the chlorine atoms Cl2 and Cl23. Indeed, if Cl23 is the axial ligand (Cu−Cl23 = 2.574(3)°) of the square pyramid, a deviation $\alpha = 25.1°$ from the perfect angle of 90° (between this bond and an idealized basal plane) is observed (see Figure S4, Supporting Information). This deviation is most likely due to the fact that this chloride anion acts as a bridging ligand, linking Cu2 to Cu3 (the angle Cu2−Cl23−Cu3 amounts to 113.0(3)°). Similarly, the chlorine atom Cl2 is out of the plane defined by the nitrogen atoms N2, N4, and N12 (Figure S4, Supporting Information; $\beta = 32.2°$). This off-plane position of Cl2 may be understood by its interaction with two pyridine rings from a neighboring pentanuclear unit (Figure S5, Supporting Information). These lone pair (lp)$\cdots\pi$ contacts[48] will be discussed in detail below. The coordination environment of Cu3 is comparable with that of Cu2. However, the CuN_3Cl_2 chromophore exhibits a coordination geometry closer to an intermediate situation, in between the square pyramid and the trigonal bipyramid ($\tau_5 = 0.42$).[45] The Cu−N and Cu−Cl bond distances (Table S1) are equivalent to reported ones.[49] Similarly to Cu2, the coordination angles reflect the strong distortion, attributable to the same structural reasons (involving the chloride atoms Cl3 and Cl23). Cu4 is the only tetracoordinated metal center of the pentanuclear complex **6** and is most likely in the +1 oxidation state (see the XAS Measurements, Magnetic Studies, and Computational Studies sections). As a result, this copper atom displays a characteristic tetrahedral geometry ($\tau_4 = 0.64$),[50] provided by two chloride atoms and two nitrogen atoms from one radical anion ligand $\mathbf{5^{MR}}$ (τ_4 describes an exact geometry of a four coordinated system; the values of τ_4 range from 1.00 for a perfect tetrahedral geometry to zero for a perfect square planar geometry).[50] The Cu−N and Cu−Cl bond lengths are typical for copper(I) species in a tetrahedral environment.[51] The angles (ranging from 77.4(3) to 145.9(2)°) around Cu4 reveal steric constraints, which clearly arise from the small bite angle of the azo-pyridine bidentate unit (N31−Cu4−N33 = 77.4(3)°), and from the participation of the chlorine atoms Cl4 and Cl4a in short intermolecular contacts. Cu5 is pentacoordinated, with a square-pyramidal geometry ($\tau_5 = 0.17$).[45] The basal plane is formed by four pyridine nitrogen atoms belonging to the two chlorinated ligands. The apical position is occupied by a chloride anion at a longer distance. The Cu−N, as well as the Cu−Cl, bond lengths lie in the normal ranges for this type of coordination.[52] The coordination angles in the basal plane are close to the ideal value of 90°, varying from 84.8(3) to 91.0(3)° (Table S1).

The crystal packing of **6** reveals interesting supramolecular interactions, which produce an intricate three-dimensional network. The pentanuclear unit is coordinated by two modified ligands $\mathbf{5^{M}}$ and $\mathbf{5^{MR}}$, which are sitting on top of each other, in a parallel manner (Figure S6, Supporting Information). The resulting intramolecular $\pi-\pi$ stacking interactions between the triazine rings is reflected by a centroid $A\cdots$centroid A' separation distance of 3.507(4) Å (Figure S6). Analogous triazine$\cdots$triazine contacts have been observed for other copper complexes with related ligands.[28,29] The coordinated pyridine rings B and B' and C and C' (Figure S7, Supporting Information) are $\pi-\pi$ interacting as well, with centroid-to-centroid distances of 3.781(5) and 3.767(5) Å, respectively. As pointed out above, the chloride atoms Cl2 (Figure S4, Supporting Information) and Cl3 are in close (binding) contacts with pyridine rings (Figure S8, Supporting Information). Indeed, a closer look at the Cl$\cdots X_{pyr}$ (where X_{pyr} symbolizes an atom of the pyridine ring) separation distances for each chloride atom reveals values (see Table S3, Supporting Information) indicative of potential lone pair$\cdots\pi$ interactions.[48,53] Thus, the Cl2$\cdots$centroid D and Cl2$\cdots$centroid D' separations are 3.559(4) and 3.307(4) Å, respectively. For Cl3, the corresponding contact distances are longer, namely, 3.985(4) Å (Cl3$\cdots$centroid E) and 4.175(4) Å (Cl3$\cdots$centroid E'). The stronger interactions noticed for Cl2 (Cl2 exhibits eight short contacts with two pyridine rings of a neighboring pentanuclear unit, while Cl3 only shows three to four interaction points) may be understood by the strong lone pair$\cdots\pi$ interaction involving the chloride atom Cl5 (Figure 2). As illustrated in Table S3, Cl5 displays short contacts with all six atoms of a triazine unit belonging to an adjacent pentanuclear complex (all distances are below 3.5 Å; Table S3). Thus, the distance between Cl5 and the centroid F of the triazine ring amounts to 3.097(4) Å. This Cl(lp)$\cdots\pi$ separation is in the range of calculated values for water−aromatic associations.[54]

(46) Gokhale, N. H.; Padhye, S. S.; Padhye, S. B.; Anson, C. E.; Powell, A. K. *Inorg. Chim. Acta* **2001**, *319*, 90–94.
(47) Folgado, J. V.; Gomezromero, P.; Sapina, F.; Beltranporter, D. *J. Chem. Soc., Dalton Trans.* **1990**, 2325–2329.
(48) Egli, M.; Sarkhel, S. *Acc. Chem. Res.* **2007**, *40*, 197–205.
(49) Cortes, R.; Lezama, L.; Delarramendi, J. I. R.; Madariaga, G.; Mesa, J. L.; Zuniga, F. J.; Rojo, T. *Inorg. Chem.* **1995**, *34*, 778–786.
(50) Yang, L.; Powell, D. R.; Houser, R. P. *Dalton Trans.* **2007**, 955–964.
(51) Bowmaker, G. A.; Healy, P. C.; Kepert, D. L.; Kildea, J. D.; Skelton, B. W.; White, A. H. *J. Chem. Soc., Dalton Trans.* **1989**, 1639–1644.
(52) Moncol, J.; Mudra, M.; Lonnecke, P.; Koman, M.; Melnik, M. *J. Chem. Crystallogr.* **2004**, *34*, 423–431.
(53) Mooibroek, T. J.; Gamez, P.; Reedijk, J. *CrystEngComm* **2008**, *10*, 1501–1515.
(54) Gallivan, J. P.; Dougherty, D. A. *Org. Lett.* **1999**, *1*, 103–105.

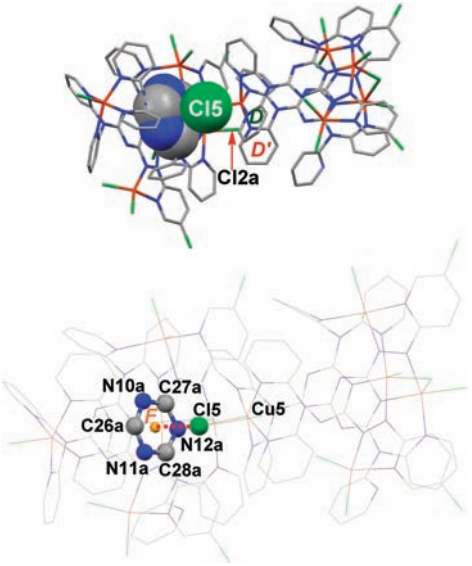

Figure 2. Lone-pair (lp)···π interactions between the chloride Cl5 and a triazine ring, *F*, of an adjacent pentanuclear complex. The distance Cl5···centroid *F* amounts to 3.097(6) Å.

As a result of this Cl5···triazine interaction, the neighboring Cl2a atom experiences increased interactions with the pyridines *D* and *D*′ (see Figures 2 and S8), in contrast to the *E*···Cl3···*E*′ association (Figure S8), which is not enhanced by any neighboring Cl(lp)···triazine(π) assembly.

Ligand Modification. As already mentioned above, the ligand dppht (**5**) undergoes significant chemical transformations upon coordination to copper, resulting in both $\mathbf{5}^{\mathbf{M}}$ and $\mathbf{5}^{\mathbf{MR}}$ (Scheme 2). The initial ligand, dppht, has been chlorinated at the para position to the hydrazino function of the pyridine ring connected to the triazine unit via the hydrazine linker (Figure 1; see chlorine atoms Cl30 and Cl40). Such copper-mediated chlorination of coordinated pyridine rings has been previously observed for other pyridine-based ligands.[55] The most fascinating feature regarding the ligand modification is found in the N2−N3 and N32−N33 bond lengths (Figure 1). Indeed, the N2−N3 bond distance is equal to 1.331(9) Å, and the N32−N33 one comes to 1.336(9) Å. The length for a NH−NH single bond is expected to be around 1.40 Å.[56,57] The value for a N=N double bond is expected to be near 1.25 Å.[58,59] The N−N bond distances for both ligands in **6** thus lie at the intermediate value, that is, 1.325 Å. Similar circumstances were observed by Kaim et al. in 1998, when they first structurally described a stable azoaromatic radical anion within a dicopper(I) complex.[26] In this crystallographic example, the N−N distance for the coordinated ligand abcp (2,2′-azobis(5-chloropyrimidine)) is 1.345 Å, which is ascribed to a radical-anion species.[26] In such a case, the intermediate bond distance results from the occupation of an antibonding π^* orbital by a single electron, as observed for other systems.[60,61] Another possibility for an intermediate N−N bond distance, for example, a bonding order of 1.5, is the partial occupation by only one electron of one of the bonding π orbitals. This situation would correspond to a neutral radical ligand, exhibiting a NH−N moiety. Nevertheless, crystallographically, it has been impossible to locate the hydrogen atom of such a NH−N moiety. Moreover, the IR spectrum of **5** does not show the presence of sharp absorption peaks around 3200 cm^{-1} and 1550 cm^{-1}, characterizing a N−H bond (see Experimental Section and Figures S1 and S2, Supporting Information). In addition, such a neutral azo-aromatic radical has so far not been observed. Moreover, overall, the combination of XAS experiments indicating at most 20% of Cu(I) species in **6** (see below), magnetic studies indicating the presence of only five spin centers of 1/2 per complex, and charge compensation considerations leads to the conclusion that only one negative charge and one spin center of 1/2 correspond to the two ligands in **6**. It thus appears that these ligands are different: one being the neutral chlorinated $\mathbf{5}^{\mathbf{M}}$ and the other being the radical anion $\mathbf{5}^{\mathbf{MR}}$. The core of complex **6** thus consists of the unit Cu^{II}_4-$Cu^{I}\mathbf{5}^{\mathbf{MR}}\mathbf{5}^{\mathbf{M}}$ which, in addition to the mentioned experimental evidence, is corroborated by theoretical calculations (see below). Although the N−N bond lengths are similar, calculations and charge considerations indicate that $\mathbf{5}^{\mathbf{MR}}$ is the ligand coordinated to the monovalent Cu4 ion. Moreover, calculations also confirm the observed long N=N bond distance for the ligand $\mathbf{5}^{\mathbf{M}}$ (the N2−N3 bond length is shorter than the N32−N33 one and is therefore closer to the value for a N=N bond). These oxidized (and deprotonated) ligands are most likely generated in situ, upon **one-electron** reduction of copper(II) to copper(I).

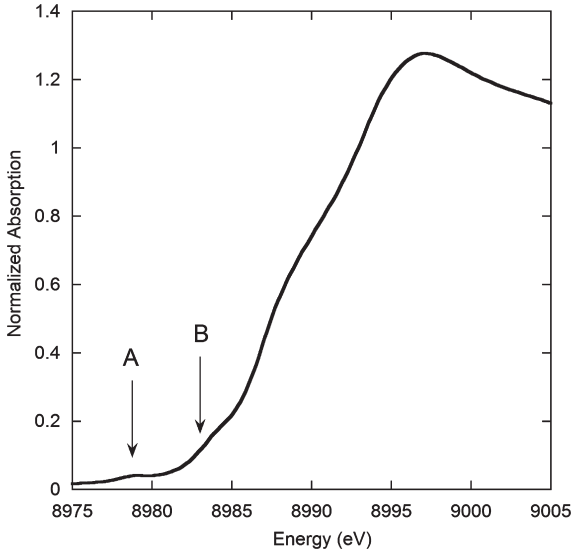

Figure 3. Normalized Cu K-edge XAS data of compound **6**, showing the presence of a small (maximally 20%) Cu(I) contribution. Arrows A and B indicate respectively 1s to 3d and 1s to 4p features (see text).

(55) Song, Y.-F.; van Albada, G. A.; Tang, J.; Mutikainen, I.; Turpeinen, U.; Massera, C.; Roubeau, O.; Sanchez Costa, J.; Gamez, P.; Reedijk, J. *Inorg. Chem.* **2007**, *46*, 4944–4950.
(56) Hosmane, R. S.; Lim, B. B.; Summers, M. F.; Siriwardane, U.; Hosmane, N. S.; Chu, S. S. C. *J. Org. Chem.* **1988**, *53*, 5309–5315.
(57) Pestana, D. C.; Power, P. P. *Inorg. Chem.* **1991**, *30*, 528–535.
(58) Bock, H.; Dienelt, R.; Schodel, H.; Van, T. T. H. *Struct. Chem.* **1998**, *9*, 279–288.
(59) Ammon, H. L.; Bhattacharjee, S. K.; Shinkai, S.; Honda, Y. *J. Am. Chem. Soc.* **1984**, *106*, 262–263.
(60) Schwach, M.; Hausen, H. D.; Kaim, W. *Inorg. Chem.* **1999**, *38*, 2242–2243.
(61) Shivakumar, M.; Pramanik, K.; Ghosh, P.; Chakravorty, A. *Inorg. Chem.* **1998**, *37*, 5968–5969.

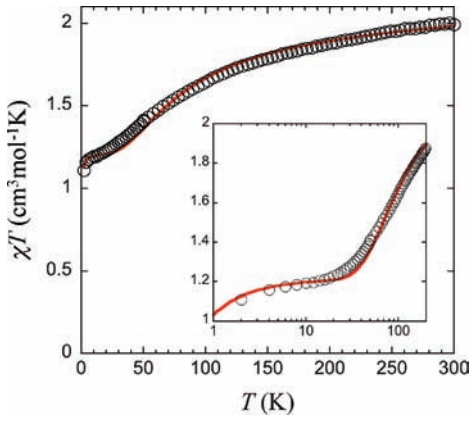

Figure 4. $\chi_M T$ vs T plot for complex **6**. Full lines represent the best fit obtained with the model described in the text. The inset gives a log-normal plot of the same data, highlighting the low-temperature area.

XAS Measurements. Figure 3 shows the normalized Cu K-edge spectrum for complex **6**. There is a weak 1s to 3d feature at ~8979 eV (arrow A in Figure 3), which is characteristic of Cu(II). In addition, there is a weak 1s to 4p shoulder at ~8983 eV (arrow B in Figure 3), which indicates the presence of a small amount of Cu(I). A comparison of these data to known Cu(I) and Cu(II) complexes shows that complex **6** is comprised of at most 20% Cu(I).[62]

Magnetic Studies. The thermal dependence of the product $\chi_M T$ (where χ_M is the molar magnetic susceptibility) is plotted in Figure 4. $\chi_M T$ gradually decreases upon lowering the temperature from 2.0 $cm^3\ mol^{-1}$ K at 300 K to reach a plateau around 1.2 $cm^3\ mol^{-1}$ K in the range 4−15 K. A further decrease is then observed down to 1.1 $cm^3\ mol^{-1}$ K at 2 K. The value near room temperature is in agreement with five uncoupled spin 1/2 centers (1.875 $cm^3\ mol^{-1}$ K for $g = 2$, see also the Supporting Information). This can correspond to (i) five Cu(II) ions; (ii) four Cu(II) ions, one Cu(I) ion, and one radical anion; or (iii) three Cu(II) ions, two Cu(I) ions, and two neutral radicals. The charge balance within the complex rules out the first possibility. This, together with the presence of Cu(I) species, as evidenced by structural and XAS data, is the reason why only the latter two hypotheses will be considered. The behavior observed is indicative of the presence of several magnetic interactions among the spin carriers, being dominated by one antiferromagnetic coupling. In the $Cu^{II}{}_3Cu^{I}{}_2$ hypothesis (with Cu4 and Cu1 being diamagnetic Cu^{I} ions), the most reasonable simulation of the experimental data (see the Supporting Information for details) indicates that the radical−radical interaction would be the dominant one, at −55(6) K. Given that the N−N moieties, where the spin density of the radical is most likely situated, are not facing each other, a direct through-space overlap of the corresponding magnetic orbital(s) is highly unlikely. Moreover, the only other radical−radical interaction pathway in the structure of **6** would be through the π-stacked triazine rings. This pathway is not expected to propagate any interaction of such strength. This therefore plays against the $Cu^{II}{}_3Cu^{I}{}_2$ possibility. Consequently, and in agreement with the XAS data and computational studies (see below), the hypothesis of a $Cu^{II}{}_4Cu^{I}$ core with one radical anion is deemed the correct one, Cu4 being the diamagnetic Cu^{I} cation. The corresponding magnetic coupling scheme would then be that illustrated in Scheme 3, which involves five different coupling constants and for which no analytical solution exists. Nonetheless, the interaction between Cu2 and Cu3 through the apical bridging chlorine (J_2) as well as those between the radical ion and Cu2 (J_4) as well as Cu1 (J_5) can reasonably be neglected. The scheme then simplifies to two exchange-coupled dimers of spin 1/2 centers with differing coupling constants, in addition to an isolated Cu^{II} ion (Cu5). The experimental data are indeed correctly reproduced with this simple model[30] (full line in Figure 4), yielding one dominant interaction of −74(4) K and one very weak one of 0.4(2) K, with a common g value of −2.07(1). The Hamiltonian used to describe each dimer was $\hat{H} = -J(S_A \cdot S_B)$, the given interaction constants being the resulting J/k_B values. A common g value was used for the five spin 1/2 centers present. The value obtained for the dominant interaction is reasonable for the Cu1···Cu2 interaction, as an interaction of −85 K was previously observed for a Cu−N−N−Cu path with a torsion angle of 151°,[63] comparable to the Cu1−Cu2 bridge in **6**. On the other hand, the weaker interaction can reasonably be ascribed to the radical ion−Cu3 interaction, although slightly stronger interactions have also been reported in the literature (for example, −3.1 K in a Cu−verdazyl complex[64]). Overall, these bulk magnetic properties indicate that **6** has a $Cu^{II}{}_4Cu^{I}$rad core, in which the dominant antiferromagnetic magnetic coupling is that between Cu1 and Cu2, through an azo N=N bridge, whereas the radical is weakly antiferromagnetically coupled to Cu3, to which it is directly coordinated. Computational studies (vide infra) confirm these considerations.

EPR Studies. X-band EPR spectra were recorded on **6** at various temperatures, from $T = 4.2$ to 280 K (Figure 5a). All of these spectra show two features, namely, one intense signal at ~3200 G with a derivative line shape with a stronger negative component and one signal at ~2200 G, also with a derivative shape. The lines are quite broad (ΔB_{pp} = 150−350 G, Figure 5b). No nitrogen hyperfine structure is resolved, thus hampering direct evidence for spin density on the ligand. Also, no copper hyperfine structure is observed. The g value of the high-field signal shifts from $g = 2.065$ at low temperatures to 2.13 at higher temperatures (Figure 5b), the latter value being common for Cu^{II}. The low-temperature g value suggests some involvement of a noncopper spin center, presumably an organic radical. Considering the model constructed on the basis of the susceptibility measurements, the EPR spectrum should be a superposition of spectra due to (i) an isolated Cu^{II} ion, (ii) a strongly coupled copper dimer, and (iii) a weakly coupled copper(II)-radical species. At low temperatures, we assume that the strongly coupled copper dimer is diamagnetic and that the EPR spectrum is due to the other two species. The main challenge is to simulate the low-field feature, and

(62) Kau, L. S.; Spirasolomon, D. J.; Pennerhahn, J. E.; Hodgson, K. O.; Solomon, E. I. *J. Am. Chem. Soc.* **1987**, *109*, 6433–6442.

(63) Grove, H.; Kelly, T. L.; Thompson, L. K.; Zhao, L. A.; Xu, Z. Q.; Abedin, T. S. M.; Miller, D. O.; Goeta, A. E.; Wilson, C.; Howard, J. A. K. *Inorg. Chem.* **2004**, *43*, 4278–4288.

(64) Barclay, T. M.; Hicks, R. G.; Lemaire, M. T.; Thompson, L. K. *Inorg. Chem.* **2003**, *42*, 2261–2267.

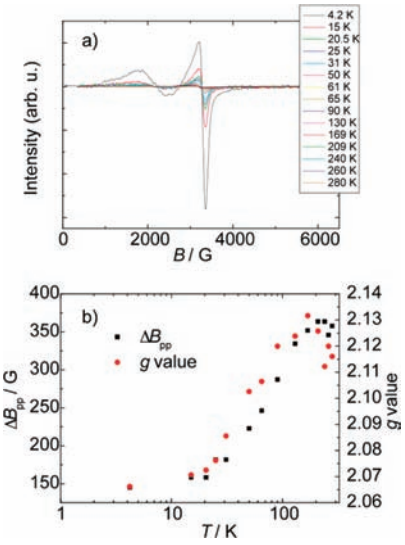

Figure 5. (a) X-band EPR spectra recorded on **6** at various temperatures, as indicated. (b) Line width (ΔB_{pp}) and g value as a function of the temperature.

we have not been successful in achieving that. The effective g value of this feature is $g \approx 3$, which is too large to be due to g value anisotropy of the copper ions. Other scenarios that could lead to such a feature are (i) a $\Delta_{ms} = 2$ half field transition within the $S = 1$ excited state of the weakly coupled copper-radical species and (ii) hyperfine- or zero-field-splitting-induced mixing between the $S = 0$ and $S = 1$ states of the same species, which allows nominally forbidden transitions from $S = 0$ to $S = 1$. The zero-field splitting would originate from the magneto−dipolar interaction between the two spins. Extensive simulations employing Easyspin[65] revealed that, whereas it is possible to reproduce the position of the low-field resonance line, neither of these scenarios can explain its intensity.

Scheme 4. The Two N−N Moieties Present in **6** According to Density Functional Theory Calculations

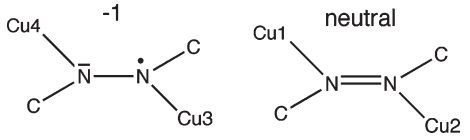

Computational Studies. We have performed calculations based on density functional theory (see the Computational Details) in order to verify the proposed electronic structure for this molecule. Due to the presence of Cu^{I} cations in this system, there are two possible models, because the magnetic properties indicate the existence of five $S = 1/2$ paramagnetic centers. Hence, a model with three Cu^{II} cations and two radicals and a second model with four Cu^{II} cations and only one radical were considered. In our calculations, we have employed starting wave functions corresponding to both models obtaining at the end of the convergence process the same model, with four Cu^{II} cations and one radical, in the two cases.

The optimization of the structure for such a model was performed, and in Figure 6, we provide the comparative superposition of this optimized structure with that

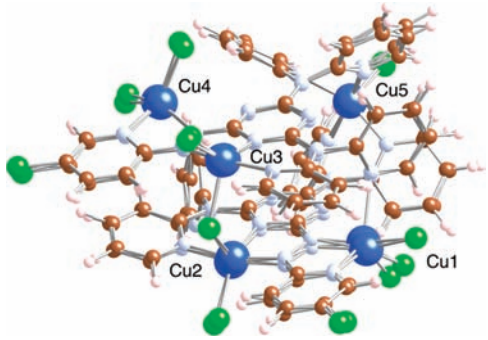

Figure 6. Superposition of the experimental structure of **6** obtained by X-ray diffraction and that corresponding to the optimization using calculations based on density functional theory.

obtained by X-ray diffraction, showing a very good agreement between them. Actually, the experimental and calculated coordination bond distances are listed and compared in Table S4 (Supporting Information), and the spin density distributions are shown in Table S5 (Supporting Information). It is then worth noting some relevant aspects in such geometrical structures, confirming the electronic structure: (i) The Cu4 metal is four-coordinate with an oxidation state of +1. (ii) The N−N bridging group between Cu4 and Cu3 shows a radical character, especially centered in the N atom coordinated to the Cu3 (spin density of 0.29 e^{-}) while the N atom coordinated to Cu4 cation adopts a non planar coordination due to the presence of a lone pair (Scheme 4). (iii) The other Cu cations (Cu1, Cu2, Cu3, and Cu5) have a formal oxidation state of +2. It is important to note that the Cu1 atom is similar to Cu4, but the rotation of a pyridine group allows [4 + 1] coordination. (iv) The N−N bridging group between Cu1 and Cu2 atoms shows an almost perfect planar geometry, both in the experimental and optimized structures, and the spin density in these N atoms is that expected for the delocalization of the spin density of the Cu^{II} cations (around +0.1 e^{-}),[66,67] in agreement with the moderate antiferromagnetic coupling propagated by the N−N bridge (see Magnetic Studies). (v) The negative charge of the radical N−N group is consistent with the neutral charge of the whole molecule. (vi) Despite the fact that a simple model (see Scheme 4) gives a different bond order for the two bridging N−N groups, the N−N distances are very similar, in agreement with the structural observations.

Concluding Remarks

The preparation of a new polydentate ligand containing a hydrazino function has allowed the synthesis of a mixed-valent $Cu^{II}_4Cu^{I}$ coordination compound, bearing an azo-based radical-anion ligand. The one-electron oxidation and deprotonation of the hydrazino-containing ligand mediated by copper(II), which is reduced to copper(I), leads to a typical azo radical-anion species, characterized by a N−N bond of around 1.33 Å. In addition, the original ligand has been monochlorinated, most likely through a copper-mediated redox process, at one of its pyridine rings. These results show

(65) Stoll, S.; Schweiger, A. *J. Magn. Reson.* **2006**, *178*, 42–55.

(66) Cano, J.; Ruiz, E.; Alvarez, S.; Verdaguer, M. *Comments Inorg. Chem.* **1998**, *20*, 27–56.

(67) Ruiz, E.; Cirera, J.; Alvarez, S. *Coord. Chem. Rev.* **2005**, *249*, 2649–2660.

that the multifunctional triazine-based ligand can accommodate both copper(II) and copper(I) ions, while the resulting Cu^{II}/Cu^{I} species features an unusual radical-anion ligand. Experimental (XAS, EPR, and magnetic susceptibility measurements) and theoretical studies (DFT) support the observed structural features.

Acknowledgment. This work has been supported financially by the Graduate Research School Combination "Catalysis", a joint activity of the graduate research schools NIOK, HRSMC, and PTN. Financial support from COST Action D35/0011, Dutch WFMO (Werkgroep Fundamenteel Materialen-Onderzoek) CW (Foundation for the Chemical Sciences), NWO, Université Bordeaux 1, CNRS, Région Aquitaine, DFG (German Science Foundation), and the DFG/CNRS bilateral program (DFG project Gu 95/59) are gratefully acknowledged. Coordination by the FP6 Network of Excellence "MAGMANet" (contract number 515767) is also kindly acknowledged. SSRL operations are funded by the DOE, BES. The SMB program is supported by the NIH, NCRR, BTP and by the DOE, BER. This publication was made possible by Grant Number 5 P41 RR001209 from the NCRR, a component of the NIH. The Generalitat de Catalunya (ICREA) is acknowledged for financial support.

Supporting Information Available: Scheme showing the ligand-based reduction of Cu^{II} to Cu^{I} species, selected bond lengths and angles and crystallographic data for **6**, figures illustrating the coordination environment around Cu2 and the supramolecular interactions occurring in the solid-state structure of **6**, table listing the short Cl···ring contact distances characterizing the lone pair···π interactions, treatment of the magnetic susceptibility data for the hypothetical $Cu^{II}{}_3Cu^{I}{}_2rad_2$ species, and data obtained by DFT calculations (Tables S4 and S5). This material is available free of charge via the Internet at http://pubs.acs.org.